Notes on the incompressible Euler equation

Daniel W. Crews

July 12, 2021

1 Ellipticity in the incompressible Navier-Stokes equation

A well-known model for the velocity field $\boldsymbol{v}$ of a viscous fluid is the Navier-Stokes equation,

$$\partial_t \boldsymbol{v} + (\boldsymbol{v} \cdot \nabla)\boldsymbol{v} = -\frac{1}{\rho}\nabla p + \nu \nabla^2 \boldsymbol{v}. \tag{1}$$

Often one specifies an equation of state for the pressure field. Alternatively, for an incompressible medium ($\nabla \cdot v = 0$) the instantaneous velocity field specifies the pressure to within a constant. Taking the divergence of Eq. 1 gives

$$\partial_t(\nabla \cdot \boldsymbol{v}) + \nabla \cdot ((\boldsymbol{v} \cdot \nabla)\boldsymbol{v}) = -\frac{1}{\rho}\nabla^2 p + \nabla \cdot (\nabla^2 \boldsymbol{v}) \tag{2}$$

which for $\nabla \cdot \boldsymbol{v} = 0$ reduces to Poisson's equation for the specific energy p/ρ

$$\nabla^2\Big(\frac{p}{\rho}\Big) = -\nabla \cdot ((\boldsymbol{v} \cdot \nabla)\boldsymbol{v}), \tag{3}$$

$$= -\partial_i v^j \partial_j v^i \tag{4}$$

where the second form of the source term is in summation-index notation [1]. In other words, the pressure field p of an incompressible fluid is an elliptic scalar field. The field source is the divergence of the velocity's convective derivative. The elliptic property means that sound (longitudinal waves) propagates instantaneously in an ideal incompressible fluid of constant density and lends a global character to solutions. Incompressible fluid waves occur in special circumstances: frame-rotation and fluid stratification produce internal, transverse waves due to Coriolis and buoyant forces.

The incompressible and inviscid limits are dynamically a coupled hyperbolic-elliptic system

$$\partial_t \boldsymbol{v} + (\boldsymbol{v} \cdot \nabla)\boldsymbol{v} = -\nabla\Big(\frac{p}{\rho}\Big), \tag{5}$$

$$\nabla^2\Big(\frac{p}{\rho}\Big) = -\partial_i v^j \partial_j v^i. \tag{6}$$

1.1 A steady solution in two dimensions

To build intuition, consider the Poisson equation for pressure in a fluid of velocity $\boldsymbol{v} = \{u, v\}$,

$$\nabla^2\Big(\frac{p}{\rho}\Big) = -(\partial_x u \partial_x u + \partial_x v \partial_y u + \partial_y u \partial_x v + \partial_y v \partial_y v). \tag{7}$$

A particular wave-like steady solution in two dimensions is the periodic velocity field

$$u(x, y) = \cos(y), \qquad v(x, y) = \sin(x) \tag{8}$$

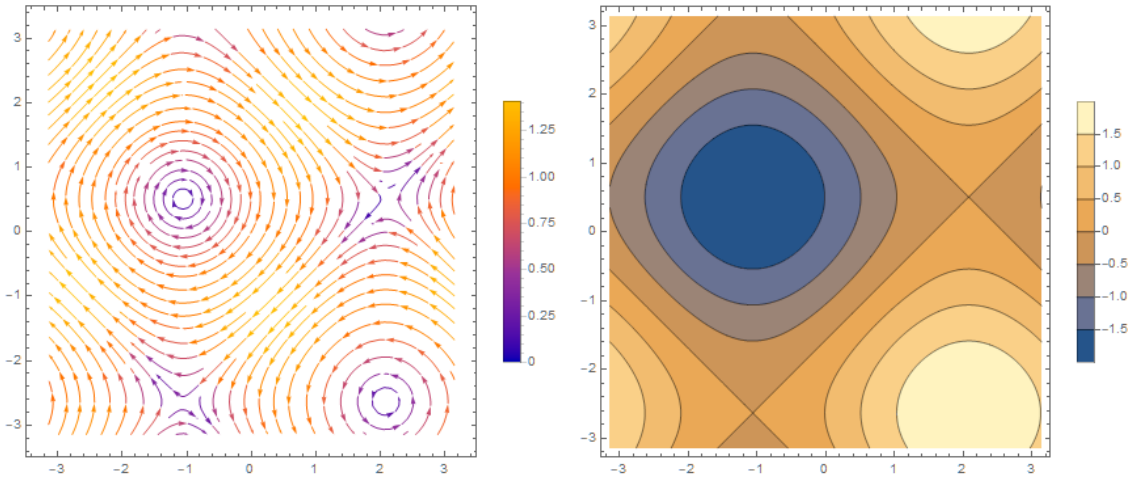

(a) Streamlines of field $\boldsymbol{v}$

(b) Field vorticity $\nabla \times \boldsymbol{v}$

Figure 1: Vector field and vorticity distribution of the steady velocity field $u = \cos(y), v = \sin(x)$. Note the presence of both hyperbolic and elliptic fixed points in the vector field, with negative vorticity within clockwise closed flux and positive vorticity within counterclockwise closed flux.

with streamlines as in Fig. 1a. The pressure field and convective derivative are

$$\frac{p(x,y)}{\rho} = -\sin(y)\cos(x), \qquad (\boldsymbol{v}\cdot\nabla)\boldsymbol{v} = \{-\sin(x)\sin(y), \cos(x)\cos(y)\}. \tag{9}$$

leading to a steady solution as the pressure gradient balances the tendency for convection,

$$\nabla\Big(\frac{p(x,y)}{\rho}\Big) = \{\sin(x)\sin(y), \cos(x)\cos(y)\} \implies (\boldsymbol{v}\cdot\nabla)\boldsymbol{v} + \nabla\Big(\frac{p(x,y)}{\rho}\Big) = 0. \tag{10}$$

The solution represents a pair of counter rotating vortices, with two elliptic and two hyperbolic fixed points. The vorticity of the prototype solution, shown in Fig. 1b, is simply

$$\omega \equiv \nabla \times \boldsymbol{v} = \cos(x) + \sin(y). \tag{11}$$

1.2 Multiple wave-number dynamics

Superpositions of Section 1.1's wave-like solutions are no longer steady as the Euler equation is nonlinear. Yet each solution of the form Eq. 8 for a given wave-number represents a vortex pattern of a particular wavenumber k_n. Thus turbulence with specified initial wavenumbers and energy transfer between modes may be observed through an initial condition such as

$$u(x,y,0) = \sum_{n=1}^{N} A_n \cos(ny + \varphi_n), \tag{12}$$

$$v(x,y,0) = \sum_{n=1}^{N} A_n \sin(nx + \varphi_n) \tag{13}$$

with φ_n a randomly sampled[1] phase factor to prevent unintentional coherence. This general initial condition has mean-zero velocity and vorticity. Initial closed flux regions can be found by inspecting the contours of the vorticity, being a sum of those of Eq. 11,

$$\omega \equiv \nabla \times \boldsymbol{v} = \sum_{n=1}^{N} nA_n(\cos(nx + \varphi_n) + \sin(ny + \varphi_n)). \tag{14}$$

1.3 Dispersion error and numerical stability

Numerical discretization introduces artificial dispersion to the incompressible Navier-Stokes equation. When fluid velocity gradients approach grid scales significant errors develop. These errors can grow exponentially and cause simulation failure through overflow.

To illustrate, consider the model problem

$$u(x, y, 0) = \cos(y + \varphi_1) + \cos(2y + \varphi_2), \tag{15}$$
$$v(x, y, 0) = \sin(x + \varphi_1) + \sin(2x + \varphi_2) \tag{16}$$

with φ_1, φ_2 random phases. The superimposed vortex pattern is shown in Fig. 2.

1.3.1 Discretization details

The Navier-Stokes equation with pressure Poisson constraint is discretized by a discontinuous Galerkin projection with seventh-order polynomials per element and the Shu-Osher third-order SSP-RK time-stepping method, while the element size $\Delta x \equiv \Delta y$ is varied depending on desired resolution. The pressure Poisson equation is solved at each RK stage using a high-order Fourier spectral method discussed in other notes. This section uses $N_x = N_y = 25$ elements per axis.

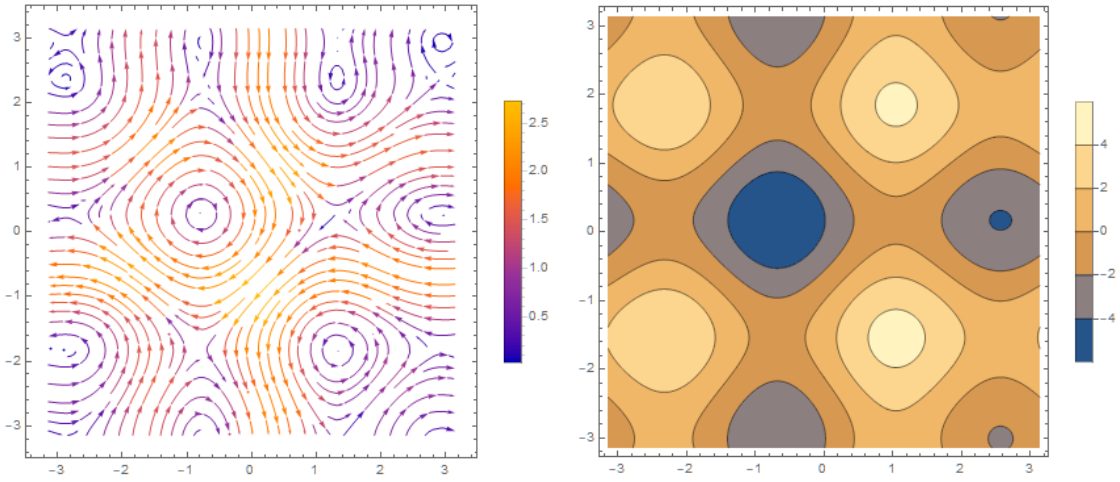

(a) Streamlines of field $\boldsymbol{v}$

(b) Field vorticity $\nabla \times \boldsymbol{v}$

Figure 2: Vector field and vorticity of the unstable vortex pattern given by Eqs. 15 and 16. The pattern mixes and evolves with time, so the initial condition is suitable to study turbulence.

[1] Each phase φ_i is chosen using the Python command `np.random.randn()` with random seed 126 and scaled by π.

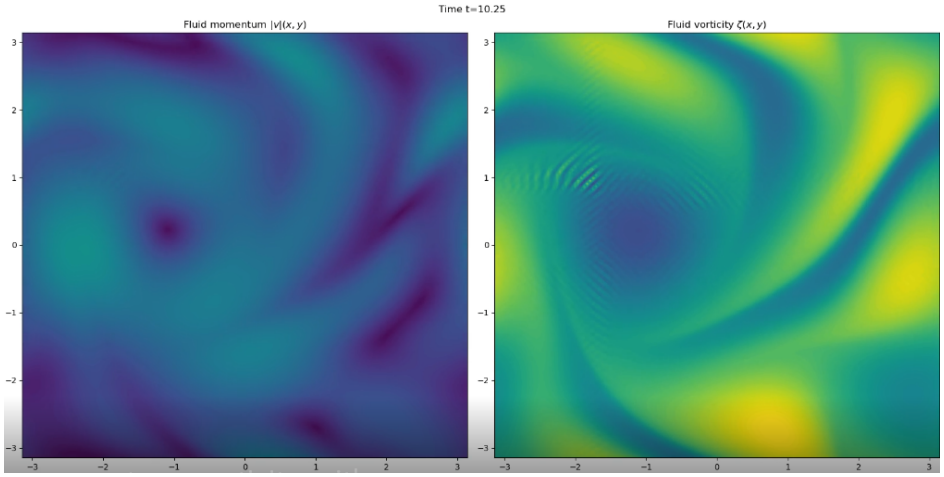

Figure 3: Errors arising within vorticity, computed during post-processing, at time $t = 10.25$.

1.3.2 Unfiltered simulations lead to solution breakdown

Running the problem with Courant numbers known to be stable for hyperbolic systems leads to solution errors, beginning first within the largest vortex, as shown in Fig. 3

The issue areas are those with the highest pressure deviation, so the development of errors is most likely related to the ellipticity of the system arising through the momentum equation's source term, the pressure gradient. The methods used are stable for purely hyperbolic systems, and this is approximated when the system is convection-dominated. Continuation of the simulation leads to breakdown as the oscillations grow exponentially.

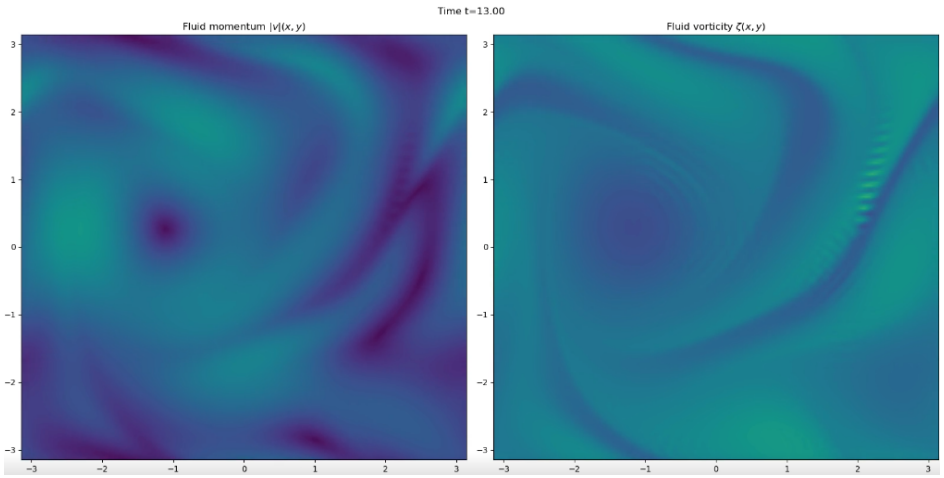

Figure 4: Filtering every timestep allows the simulation to progress past $t = 10$. However, errors arising due to filtering arise at a later time, here $t = 13$.

1.3.3 Filtering is stabilizing, but overfiltering is destabilizing

The errors consist of sub-grid scale, or aliased, wavelengths. These wavelengths may be filtered out of the solution. A spectral filtering method consists of transforming to a global Fourier basis and

then inverting the transform, *i.e.* summing the Fourier series, up to the grid scale,

$$\widehat{\boldsymbol{u}}_{p,q} = \int_{-\infty}^{\infty}\int_{-\infty}^{\infty} \boldsymbol{u}(x,y)e^{-i(k_{x,p}x+k_{y,q}y)}dxdy, \quad \boldsymbol{u}(x,y) \approx \sum_{p,q=-G}^{G} \widehat{\boldsymbol{u}}_{p,q}e^{i(k_{x,p}x+k_{y,q}y)} \tag{17}$$

with $G = \frac{2\pi}{\Delta x}$ the grid wavenumber. This has been discussed in prior notes for the LGL basis.

Application of the filter at each time-step is initially stabilizing, but at later times leads to a different sort of error as shown in Fig. 4. The filter introduces oscillations at sharp gradients approaching the grid scale, so produces oscillatory errors in regions of filamentation.

1.3.4 Moderate filtering is simply stabilizing

Rather than apply the filter to the velocity field every time-step, it can be applied every so many time-steps. Doing this for every 75 time-steps is seen to be more stabilizing than filtration at each step, shown in Fig. 5. By this method the simulation can be carried out to $t = 20$ before noticeable dispersion error arises.

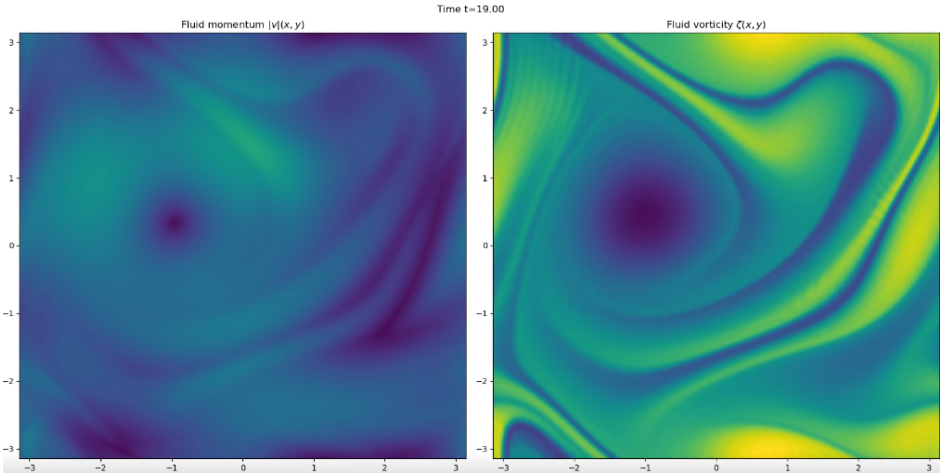

Figure 5: Filtration at a moderate interval of timesteps is greatly stabilizing. In this example, filtration every 75 timesteps allows the simulation to progress to $t = 19$ with moderate error.

1.3.5 Filamentation of vorticity

As the turbulent flow develops, the small flow velocity along the streamlines emanating from the hyperbolic fixed points leads to filamentary structures. One way to understand this is by the vorticity equation (the momentum equation's curl with $\boldsymbol{\omega} \equiv \nabla \times \boldsymbol{v}$),

$$\frac{d\boldsymbol{\omega}}{dt} = (\boldsymbol{\omega} \cdot \nabla)\boldsymbol{v} \tag{18}$$

with the source term representing vortex stretching by fluid motions. Yet in two dimensions, the curl is simply a pseudoscalar and $\omega \cdot \nabla$ is formally zero, making vorticity a Lagrangian constant.

2 Numerical methods

This section details some approximation tools used to solve Eq. 1 and explores a novel technique to incorporate the viscous term $\nu\nabla^2\boldsymbol{v}$. Generally, the Navier-Stokes equation is a convection-dominated parabolic PDE. With the incompressibility constraint, the pressure Poisson equation makes the over-all system elliptic. However in most cases, the system is still convection-dominated, which is to say that for small times Δt motion along characteristic curves accounts for most of the fluid evolution. The discontinuous Galerkin (DG) method is ideal for discretization of the nonlinear first-order differential terms responsible for convection.

On the other hand, discretization of the second-order terms, namely the Laplacian operator within the diffusion term $\nu\nabla^2\boldsymbol{v}$ and the Poisson equation for pressure, is more troublesome in DG. The local discontinuous Galerkin method is a typical approach for second-order derivatives, yet is time-consuming to implement, introduces an additional set of variables for the vector gradient, and has less intuitive numerical fluxes than for DG applied to first-order PDEs. An alternative and common approach to approximation of the Laplacian utilizes spectral methods, as it is a linear differential operator. Yet Fourier spectral methods are usually restricted to equally-spaced grids.

For this reason, this section describes a Galerkin projection approximation of the incompressible Navier-Stokes equation by connecting the DG method's quadrature points to the Fourier basis of the global domain. That is, the convective nonlinear flux divergence $\nabla\cdot(\boldsymbol{v}\boldsymbol{v})$ is discretized with the DG method, while all terms linear in derivatives are approximated using a high-order quadrature-based Fourier spectral method.

2.1 The discontinuous Galerkin projection

The system is integrated against a set of test functions $\boldsymbol{\psi}_k$ spanning the approximation space,

$$\langle\partial_t\boldsymbol{v}+\nabla\cdot(\boldsymbol{v}\boldsymbol{v})|\boldsymbol{\psi}_k\rangle=\langle-\frac{1}{\rho}\nabla p+\nabla^2\boldsymbol{v}|\boldsymbol{\psi}_k\rangle \tag{19}$$

$$\langle\nabla^2 p|\psi_k\rangle=-\langle\rho\partial_i v^j\partial_j v^i|\psi_k\rangle \tag{20}$$

and the following variables are projected into the same approximation space, with expansions

$$\boldsymbol{v}=\sum_{\ell=1}^{N}\boldsymbol{v}^\ell\boldsymbol{\psi}_\ell,\qquad \nabla\boldsymbol{v}=\sum_{\ell=1}^{N}(\nabla\boldsymbol{v})^\ell\boldsymbol{\psi}_\ell\qquad \nabla^2\boldsymbol{v}=\sum_{\ell=1}^{N}(\nabla^2\boldsymbol{v})^\ell\boldsymbol{\psi}_\ell, \tag{21}$$

$$p=\sum_{\ell=1}^{N}p^\ell\psi_\ell,\qquad \nabla p=\sum_{\ell=1}^{N}(\nabla p)^\ell\boldsymbol{\psi}_\ell,\qquad \nabla^2 p=\sum_{\ell=1}^{N}(\nabla^2 p)^\ell\psi_\ell. \tag{22}$$

The basic idea is that rather than defining one auxiliary variable $q=\nabla\boldsymbol{v}$ as in the LDG method, instead all gradient variables are explicitly defined and expanded in the projection basis. Then, the piecewise polynomial basis ψ is connected to a global basis, *e.g.* the Fourier basis e^{ikx},

$$p=\sum_{\ell=1}^{N}p^\ell\psi_\ell\approx\sum_{m=-\Delta x//L}^{\Delta x//L}c^m\exp\left(i\boldsymbol{k}_m\cdot\boldsymbol{x}\right) \tag{23}$$

via an array $\mathbb{T}$ consisting of the *connection coefficients* of the two bases[2],

$$c^m=\mathbb{T}^m_\ell p^\ell. \tag{24}$$

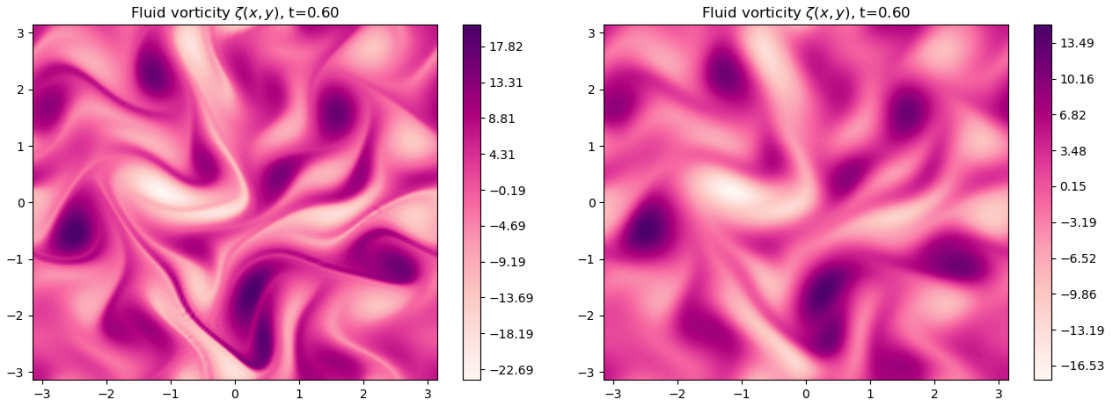

(a) Viscosity $\nu = 0$ (b) Viscosity $\nu = 0.03$

Figure 6: Comparison of inviscid and viscous flows by filled contours of vorticity in a flow with initialized modes $k = 1, 2, 3$, and 4 up to time $t = 0.6$. The addition of the viscous term point-wise to the semi-discrete ODE is simulation-stabilizing by smoothing sharp gradients as they approach grid lengths, or aliased scales.

By passing to the Fourier basis, a quadrature-integrated approximation to the derivatives may then be determined, accurate to the same order as the piecewise interpolation polynomial basis. Transforming back to the basis ψ by summing the Fourier coefficients connects the expansion coefficients of p, ∇p, and $\nabla^2 p$ by elementary arithmetic operations. As an example, the pressure gradient and Laplacian coefficients are connected to the pressure coefficients by

$$(\nabla p)^\ell = \sum_{m=-\Delta x//L}^{\Delta x//L} i\boldsymbol{k}_m (\mathbb{T}_\ell^m p^\ell) \exp\left(i\boldsymbol{k}_m \cdot \boldsymbol{x}\right) \tag{25}$$

$$(\nabla^2 p)^\ell = \sum_{m=-\Delta x//L}^{\Delta x//L} -(\boldsymbol{k}_m \cdot \boldsymbol{k}_m)(\mathbb{T}_\ell^m p^\ell) \exp\left(i\boldsymbol{k}_m \cdot \boldsymbol{x}\right) \tag{26}$$

The very same considerations hold for the coefficients $(\nabla \boldsymbol{v})^\ell$ and $(\nabla^2 \boldsymbol{v})^\ell$, simply generalized to the vector case. These approximations are then applied pointwise in the semi-discrete equation for timestepping. For example, having discretized the flux divergence $\nabla \cdot (\mathcal{F})$ with the usual DG method, where $\mathcal{F} \equiv \boldsymbol{v}\boldsymbol{v}$, the weak form semi-discrete equation is

$$\frac{d\boldsymbol{v}^\ell}{dt} = \Upsilon \mathcal{F}^\ell - \Xi \mathcal{F}^{*,\ell} - (\nabla p)^\ell + (\nabla^2 \boldsymbol{v})^\ell \tag{27}$$

because the matrix coefficients of the auxiliary variables following Galerkin projection are the mass matrix. Since the Fourier derivative approximations are accurate to the chosen quadrature order, this method can be called a mixed high-order spectral/DG method. Remaining work is to characterize explicit timestepping limitations due to viscostiy.

References

[1] C. Hirsch. *Numerical Computation of Internal & External Flows*, volume 1. Butterworth-Heinemann, Second edition, 2007.

[2] S. Olver, R.M. Slevinsky, and A. Townsend. Fast algorithms using orthogonal polynomials. *Acta Numerica*, 29:573–699, 2020.